

Hyperbolic Heat Transfer Equation for Radiofrequency Heating: Comparison between Analytical and COMSOL solutions

V. Romero-García¹, M. Trujillo^{*2}, M. J. Rivera², J. A. López Molina², and E. J. Berjano³

¹Centro de Tecnologías Físicas: Acústica, Universidad Politécnica de Valencia,

²Dpto. Matemática Aplicada. Instituto Universitario de Matemática Pura y Aplicada, Universidad Politécnica de Valencia,

³Institute for Research and Innovation on Bioengineering (I3BH), Universidad Politécnica de Valencia

*Escuela Técnica Superior de Arquitectura,

Dpto. Matemática Aplicada. Universidad Politécnica de Valencia.

Camino de Vera s/n. 46022. Valencia. SPAIN

matrugui@mat.upv.es

Abstract: The radiofrequency heating (RFH) is widely employed to heat biological tissue in different surgical procedures. Most models analyze the RFH employing a parabolic heat transfer equation (PHTE) based on Fourier's theory. The PHTE can be used for problems involving long heating times or low thermal gradients. However, when the problem involves short heating times or extreme thermal gradients it is needed to solve it using the hyperbolic heat transfer equation (HHTE), where a wavy behavior of heat conduction with a finite thermal propagation speed is assumed. We have recently proposed a model to study the temperatures profiles which are produced in biological tissue when it is heated by RF introducing the effect of the blood perfusion. The electrical-thermal coupled problem has been analytically solved by using the HHTE. COMSOL Multiphysics can be used to solve this kind of problems numerically. We compare the results obtained by COMSOL with those obtained by the analytical solution of the problem.

Keywords: Hyperbolic heat equation, parabolic heat transfer equation, radiofrequency heating, radiofrequency ablation.

1 Introduction

Radiofrequency heating (RFH) has been employed in a multitude of minimally intrusive operational techniques in the modern surgery. Changing the corneal curvature to correct refractive errors [14], the elimination of cardiac arrhythmias [3] and thermal destruction of tumors [15] are examples of application of RFH. RFH is based on the point heating of target zones of human tissue in which a great amount

of heat is transferred on a very small time scale.

The equation for the thermal current conservation with a given internal heat source $S(\mathbf{x}, t)$,

$$\nabla \cdot \mathbf{q}(\mathbf{x}, t) + \frac{k}{\alpha} \frac{\partial T}{\partial t}(\mathbf{x}, t) = S(\mathbf{x}, t), \quad (1)$$

is generally used as the fundamental relation to model the heat transfer. $\mathbf{q}(\mathbf{x}, t)$ represents the thermal flux and $T(\mathbf{x}, t)$ is the temperature at point $\mathbf{x} \in D$ in the biological tissue domain $D \subset \mathbb{R}^3$ at time $t \in \mathbb{R}_+$, figure 1; k denotes the thermal conductivity and $\alpha = \frac{k}{\eta c}$ is the diffusivity, where η is the density and c is the specific heat of the material under consideration. The product ρc is the well known volumetric heat capacity. The explicit decomposition of the internal heat sources, $S(\mathbf{x}, t)$, was introduced by Pennes [10] in the bioheat equation.

Traditionally, the thermal flux term of equation (1) has been modelled by the Fourier's theory, $\mathbf{q}(\mathbf{x}, t) = -k\nabla T(\mathbf{x}, t)$, then (1) is a parabolic heat transfer equation (PHTE). In this case, an infinite thermal energy propagation speed is assumed, which produces that any local temperature disturbance causes an instantaneous perturbation in the temperature in the medium [4]. This model is specially used for modelling the heating of biological tissue in the case of long heating time or low thermal gradients.

At the present, the minimally intrusive operational techniques in the modern surgery consist in RFH on very small time scales where high thermal gradients are allowed. For this cases the classical model (PHTE) fails [9], then it seems necessary an alternative theory with a finite thermal propagation speed for describing these phenomena. For these reasons the

interest of solving heat transfer problems with an hyperbolic heat transfer equation (HHTE) has increased in the last years [5, 13].

The general form of the hyperbolic heat transfer equation (HHTE) is (see [9])

$$-\Delta T(\mathbf{x}, t) + \frac{1}{\alpha} \left(\frac{\partial T}{\partial t}(\mathbf{x}, t) + \tau \frac{\partial^2 T}{\partial t^2}(\mathbf{x}, t) \right) = \frac{1}{k} \left(S(\mathbf{x}, t) + \tau \frac{\partial S}{\partial t}(\mathbf{x}, t) \right) \quad (2)$$

where τ is the thermal relaxation time. k, η, c and τ are assumed to be constants. Note that PHTE, equation (1) is obtained if we consider $\tau = 0$ in (2), i.e. infinite thermal energy propagation speed.

Unfortunately the vast majority of heat transfer problems that arise from real and practical situations involves complex geometries, unusual initial or boundary conditions, or they are non-linear problems. These conditions lead us to use numerical methods for solving them. Among a widespread numerical methods, the Finite Element Method (FEM) and the Finite Differences Method seem a good candidates to solve these real and practical problems. In this work we use COMSOL Multiphysics.

Until now different problems about the RFH of biological tissue without considering blood perfusion have been solved [5, 7, 6]. The goal of this paper is the numerical study, according to the HHTE, of the temperature profiles produced in the biological tissue when RFH is applied taking into account the effect of the blood perfusion. The comparison of the numerical with the analytical results is also shown in this work.

2 Theoretical Modelling

Consider a spherical active electrode completely embedded in the biological tissue. The radius of the electrode is r_0 . The tissue is considered homogeneous with infinite dimensions and the dispersive electrode to be placed at the infinity. Due to the geometry model we use spherical coordinates, and as the model presents radial symmetry, an one-dimensional approach is possible, r being the dimensional variable. Consequently, the model domain is restricted to the biological tissue, i.e. the electrode body is not included in the model. In figure 1 a schematic view of the problem is shown.

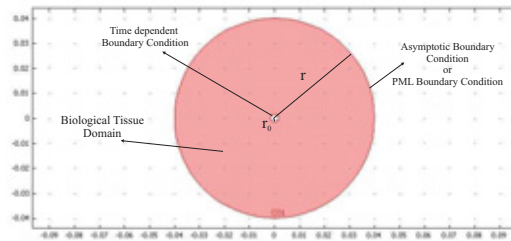


Figure 1: Schematic view of the problem. r_0 is the radius of the electrode and r is the radius of the tissue domain.

The infinite dimensions of the biological tissue will be analyzed considering a biological tissue domain big enough to neglect the reflections produced by the exterior boundary in the region near the electrode (asymptotic boundary condition). We use the PDE coefficient form with time dependent solver in order to implement all the previous equations in COMSOL. We have made different sensibility analysis based on the time step. In order to compare the numerical results with the analytical ones we need to apply both solutions to a specific case. As biological tissue we have chosen the liver.

2.1 Governing Equation

The general expression of the HHTE can be seen in equation (2). We have to define the internal heat sources according to the problem we want to solve in this work. The bioheat equation [10] provides us the explicit decomposition of the internal sources,

$$S(\mathbf{x}, t) = S_s(\mathbf{x}, t) + S_p(\mathbf{x}, t) + S_m(\mathbf{x}, t), \quad (3)$$

where the subindex s denotes a surgical heat source (e.g. laser or radiofrequency treatment), p refers to blood perfusion, and m to any source related to metabolic activity. In our problem the source term for the RFH modeling (i.e. the Joule heat produced per unit volume of tissue, $S_s(r, t)$) can be expressed as [2]:

$$S_s(r, t) = \frac{P r_0}{4 \pi r^4} H(t) \quad (4)$$

where P is the total applied power (W) and $H(t)$ is the Heaviside function, which allows

to model the power application by means of a step at $t = 0$. And the source term related to blood perfusion can be expressed as [10]:

$$S_m(r, t) = -\eta_b c_b w_b (T - T_0) \quad (5)$$

where η_b is the density of the blood, c_b the specific heat of the blood, w_b is the perfusion blood flux and T_0 is the supposed constant blood temperature. In our case we do not consider internal heat sources related to metabolic activity.

Introducing (4) and (5) in the expression of equation (2) in spherical coordinates the resulting governing equation is

$$\begin{aligned} & -\alpha \left(\frac{\partial^2 T}{\partial r^2}(r, t) + \frac{2}{r} \frac{\partial T}{\partial r}(r, t) \right) + \\ & \quad \zeta \frac{\partial T}{\partial t}(r, t) + \tau \frac{\partial^2 T}{\partial t^2} \\ = & \frac{P \alpha r_0}{4 \pi k r^4} \left(H(t) + \tau \delta(t) \right) - B(T - T_0) \quad (6) \end{aligned}$$

where $\delta(t)$ is Dirac's function, $B = \frac{\alpha \eta_b c_b w_b}{k}$ and $\zeta = 1 + \tau B$.

2.2 Initial and Boundary Conditions

The initial conditions are

$$T(r, 0) = T_0, \quad \frac{\partial T}{\partial t}(r, 0) = 0, \quad \forall r > r_0 \quad (7)$$

where T_0 is the initial temperature (i.e. tissue temperature before heating). We use the same symbol than for the blood temperature since both are equal.

Respect to the boundary conditions

$$\lim_{r \rightarrow \infty} T(r, t) = T_0 \quad \forall t > 0. \quad (8)$$

To write the boundary condition at $r = r_0$ we shall adopt a simplification assuming the thermal conductivity of the electrode is more larger than that of the tissue (i.e. assuming that the boundary condition at the interface between electrode and tissue is mainly governed by the thermal inertia of the electrode) [2]. After some algebraic modifications, the boundary condition in $r = r_0$ can be written as

$$\begin{aligned} & \frac{\tau \eta_0 c_0 r_0}{3 k} \left(\frac{1}{\tau} \frac{\partial T}{\partial t}(r_0, t) + \frac{\partial^2 T}{\partial t^2}(r_0, t) \right) \\ & = \frac{\partial T}{\partial r}(r_0, t). \quad (9) \end{aligned}$$

3 Use of COMSOL Multiphysics

In this paper the numerical simulation has been performed using COMSOL Multiphysics software version 3.2b. COMSOL presents several models to solve a wide range of PDEs. In our case we have chosen a two-dimensional problem using the *PDE coefficient Form* option for a *Time-dependent analysis, wave type*. As we mentioned, for the case of the analytical solution, the model can be solve easily assuming radial symmetry, i.e. 1D analysis. However, we prefer a 2D analysis for our problem since it is more visual than a 1D solution and the solution obtained takes a similar computational time. The use of a 2D geometry, instead of the 1D geometry, does not mean any significant change in the problem. The problem geometry can easily drawn with the CAD tools of COMSOL, see figure 1.

Using the different menus of COMSOL we can introduce the governing equation (6). In order to obtain a numerical model of the analytical one introduced in last sections, we have used the coefficient expression of PDE problem in COMSOL. We can introduce easily the proper parameters of our model. Analogously to the analytical model, we used the source term in equations (4) and (5), the initial conditions (7) and the boundary conditions (8) and (9). In the case of the Heaviside and delta's functions of the governing equation we used the COMSOL functions *flc2hs(t, p)* [1] and *fldc2hs(t, q)*, respectively. Exactly, $y = flc2hs(x, p)$ computes the values of a smoothed version of the Heaviside function $y = (x > 0)$, the function is 0 for $x < -p$, and 1 for $x > p$. By a sensibility analysis we chose $p = 0.01$ and $q = 0.05$.

The automatic mesh generated by COMSOL is enough to obtain the solution. The mesh is formed with triangular elements. We made a sensibility analysis and checked that a more refinished meshes did not produce results closer to the analytical ones.

Finally, the Solver of COMSOL must be configured taking into account the temporal characteristics of the analysis. The maximum time interval used was $t \in [0, 180]$ s. For a sensibility analysis we chose in the *General* menu a time-step of 1 s and from the *Time Stepping* menu we selected that the times to store in output are the times steps from the solver. The times steps taken by the solver were be

chosen “strict”.

4 Physical parameters

In this work we have solved the problem considering liver as biological tissue, and the physical properties shown in Table 1 for the blood and the electrode.

Physical property	Liver	Blood	Electrode
Density			
η (kg/m^3)	1060	1000	21500
Specific heat			
c ($J/kg \cdot K$)	3600	4148	132
Conductivity			
k ($W/m \cdot K$)	0.502		

Table 1: Physical properties of the Liver, blood and electrode used in this work.

In the case of the perfusion coefficient w_b we used two values: $w_b = 0$ (corresponds to the case without perfusion) and $w_b = 0.01 s^{-1}$. The blood and tissue initial temperatures were the same $T_0 = 37$ °C. The applied power was of $P = 1$ W.

There is a lack of experimental data regarding the thermal relaxation time τ of biological tissue. In fact, although Mitra *et al* found a value of $\tau = 16$ s in processed meat [8], no values have been measured for non excised tissues, which are the usual radiofrequency ablation target (heart, liver or cornea). For this reason we assumed two different values of 16 s from [8] and 1 s from [12].

In the case of geometrical parameters, in this work r_0 is considered 0.0015 m. The value of r has been chosen as $R = 0.4$ m from a sensibility analysis. In this analysis we have taking into account that the R value does not affect the solution obtained, and neither be unnecessarily too large.

5 Results

The analytical solution of the HHTE without considering the perfusion term has been analyzed in previous works [5, 7, 6]. In a re-

cent work we have studied the RFH in biological tissue using HHTE including the perfusion term [11]. In this work we obtain the numerical solution of equation (2) considering the perfusion term by means of COMSOL. We will compare the analytical and the numerical results.

5.1 Analytical and Numerical Solutions

The temperature evolution evaluated in the point $x = 2r_0$ has been obtained both analytically and numerically for two heating times, 60 s and 180 s, and for two different values of the thermal relaxation time $\tau = 16$ and $\tau = 1$ s. We have also obtained the value of the temperature evolution without perfusion, $w_b = 0 s^{-1}$, in order to compare the results with the case where perfusion is considered, $w_b = 0.01 s^{-1}$.

As we have mentioned above we solve a 1D problem analytically, however numerically we solve a 2D problem with axial symmetry. Figure 2 shows the temperature profiles obtained numerically. The color scale represents the temperature in degrees Celcius (°C) and the graph is obtained considering perfusion $w_b = 0.01 s^{-1}$ and the relaxation time $\tau = 1$ s. The graph correspond to temperature distribution in the biological tissue at the instant $t = 60$.

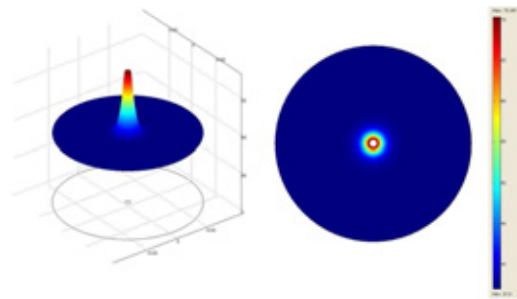


Figure 2: 2D and 3D temperature profiles processed by COMSOL at $t = 60$ s in the biological tissue with perfusion ($w_b = 0.01 s^{-1}$) and $\tau = 1$ s.

Figure 3 shows the temperature evolution until $t = 60$ s (A) and until $t = 180$ s (B) at point $x = 2r_0$. The dashed line corresponds to the case with perfusion ($w_b = 0.01 s^{-1}$) and the continuous line to the case without perfusion ($w_b = 0 s^{-1}$). Both graphics (A) and (B) were obtained using the numerical solution with two different values of the thermal

relaxation time ($\tau = 16$ and $\tau = 1$ s). The lines shown in these graphs correspond to a cross-section of the 2D solution provided by the numerical model.

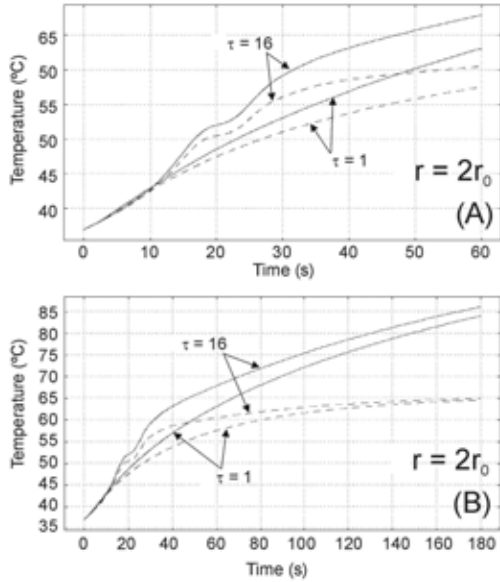


Figure 3: Numerical results at point $x = 2r_0$ with perfusion (dashed line, $\omega_b = 0.01 \text{ s}^{-1}$) and without perfusion (continuous line, $\omega_b = 0 \text{ s}^{-1}$) obtained using the numerical solution with two different values of the thermal relaxation time $\tau = 16$ and $\tau = 1$ s. (A) until 60 s, (B) until 180 s.

The analogous analytical results of the figure 3 are shown in figure 4. Dashed line represents the analytical results for the case without perfusion. The result considering perfusion is represented with continuous line.

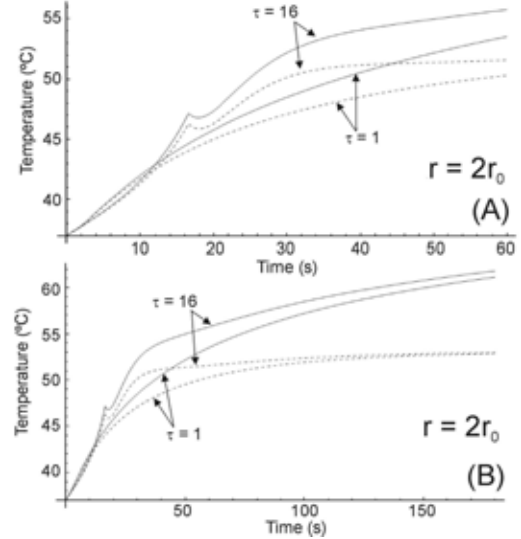


Figure 4: Analytical results at point $x = 2r_0$ with perfusion (dashed line, $\omega_b = 0.01 \text{ s}^{-1}$) and without perfusion (continuous line, $\omega_b = 0 \text{ s}^{-1}$) obtained using the numerical solution with two different values of the thermal relaxation time $\tau = 16$ and $\tau = 1$ s. (A) until 60 s, (B) until 180 s.

6 Discussion

6.1 Singularities

One of the most remarkable characteristic of the solution of the HHTE is the presence of cuspidal-type singularities [6]. This is a temperature peak which travel through the medium at finite speed. These peaks cannot be observed in the solution from the PHTE.

In figure 4 we can observe the presence of these singularities in the analytical solution. A very satisfactory characteristic of the numerical solution is that it also shows the singularities found in the analytical solutions of the HHTE. This fact can be clearly seen in figure 3. We observe the singularity at the same time. As we expect for the numerical solution the temperature peak is smoothed. Indeed, we had to change some automatic options of the COMSOL solver in order to observe the temperature peak. Specifically, the times to store in output must be the times steps from the solver. We have marked as “strict” the time steps taken by the solver.

6.2 Effect of the blood perfusion

Our previous works [5], [7] and [13] based on the study of RFH in biological tissue using HHTE did not include the perfusion term. In the present study we added this term. Comparing the graphics obtained with and without perfusion ($w_b = 0.01$ and $w_b = 0 \text{ s}^{-1}$) we can conclude that considering the perfusion term the temperatures obtained are lower than those predicted by the solution without perfusion.

6.3 Analytical versus Numerical solution

If we compare figures 3(A) and 4(A) we observe that the behavior of both solutions at point $x = r_0$ is practically identical. However, there exist differences in temperatures in all the cases. These differences increase with the time: at time $t = 10 \text{ s}$ there exist not significant differences between both solutions (≈ 2 or $3 \text{ }^\circ\text{C}$), at $t = 20 \text{ s}$ the differences have increased ($\approx 5 \text{ }^\circ\text{C}$) and at $t = 60 \text{ s}$ there exist considerable differences ($\approx 13 \text{ }^\circ\text{C}$). We do not have a clear reason to explain this fact. However, we suspect that it is related with the error that is implicit in all the numerical solutions. In this way, this error is small at the beginning of the heat process and with every time step it is increasing. We have checked that further the considered point is, lower the differences are.

7 Conclusion

In this work we have obtained the numerical solution of the RFH of biological tissue using the HHTE by means of software COMSOL Multiphysics. We can also observe that COMSOL can be used to solve the HHTE similarly as in the case of the analytical model. This numerical solution opens the possibilities to analyze the HHTE in more realistic cases as for example more complicated geometries (more realistic electrode and tissue geometries with irregular boundaries) or different thermal characteristics of the problem.

References

[1] Y. Bilotsky and M. Gasik, *Modelling multilayer systems with time-dependent heat source and new transition functions*, Pro-

ceedings of the 2006 Nordic COMSOL Conference.

- [2] A. Erez and A. Shitzer, *Controlled destruction and temperature distributions in biological tissues subjected to monoactive electrocoagulation*, *J. Biomech. Eng.* **102** (1980), 42–49.
- [3] A.S. Geha and K. Abdelhady, *Current status of the surgical treatment of atrial fibrillation*, *World J. Surg.* **32** (2008), 46–49.
- [4] J. Liu, X. Chen, and L.X. Xu, *New thermal wave aspects on burn evaluation of skin subjected to instantaneous heating*, *IEEE Trans. Biomed. Eng.* **46** (1999), 420–428.
- [5] J.A. López Molina, M.J. Rivera, M. Trujillo, and E.J. Berjano, *Effect of the thermal wave in radiofrequency ablation modeling: an analytical study*, *Phys. Med. Biol.* **53** (2008), 1447–1462.
- [6] J.A. López Molina, M.J. Rivera, M. Trujillo, and E.J. Berjano, *Thermal modeling for pulsed radiofrequency ablation: Analytical based on hyperbolic heat equation*, *Med. Phys.* **36** (2008), no. 4, 1112–1119.
- [7] J.A. López Molina, M.J. Rivera, M. Trujillo, F. Burdío, J.L. Lequerica, F. Hornero, and E.J. Berjano, *Assessment of hyperbolic heat transfer equation in theoretical modeling for radiofrequency heating techniques*, *Open Biomed. Eng. J.* **2** (2008), 22–27.
- [8] K. Mitra, S. Kumar, A. Vedavarz, and M.K. Moallemi, *Experimental evidence of hyperbolic heat conduction in processes meat*, *J. Heat Transfer* **117** (1995), 568–573.
- [9] M.N. Ozisik and D.T. Tzou, *On the wave theory in heat conduction*, *J. Heat Transfer* **116** (1994), 526–535.
- [10] H.H. Pennes, *Analysis of tissue and arterial blood temperatures in the resting human forearm*, *J. Appl. Physiol.* **85** (1998), no. 1, 5–34.
- [11] M.J. Rivera, M. Trujillo, J.A. López Molina, V. Romero-García, and E.J. Berjano, *Modeling the radiofrequency ablation of the biological tissue*

using the hiperbolic heat equation: Analytical and numerical solution, Submitted to Physics in Medicine and Biology.

- [12] T.C. Shih, H.S. Kou, C.T. Liauh, and W.L. Lin, *The impact of thermal wave characteristics on thermal dose distribution during thermal therapy: a numerical study*, Med. Phys. **32** (2005), no. 9, 3029–3036.
- [13] M.M. Tung, M. Trujillo, J.A. López Molina, M.J. Rivera, and E.J. Berjano, *Modeling the heating of biological tissue based on the hyperbolic heat transfer equation*, Mathematical and Computer Modeling **50** (2009), 665–672.
- [14] G.O. Waring 4th and D.S. Durrie, *Emerg-*

ing trends for procedure selection in contemporary refractive surgery: consecutive review of 200 cases from a single center, J. Refract. Surg. **24** (2008), 419–423.

- [15] J.C. Zhu, T.D. Yan, and D.L. Morris, *A systematic review of radiofrequency ablation for lung tumors*, Ann. Surg. Oncol. **15** (2008), 1765–1774.

Acknowledgements

This work received financial support from the Spanish “Plan Nacional de I+D+I del Ministerio de Ciencia e Innovación” (Grant No. TEC2008-01369/TEC) and from the MEC and FEDER Projects No. MTM2007-64222 and MAT2009-09438.